Advances in Brief

Analysis of the Phosphatidylinositol 3′-Kinase Signaling Pathway in Glioblastoma Patients *in Vivo*[1]

Gheeyoung Choe,[2] Steve Horvath,[2] Timothy F. Cloughesy, Katherine Crosby, David Seligson, Aarno Palotie, Landon Inge, Bradley L. Smith, Charles L. Sawyers, and Paul S. Mischel[3]

Departments of Pathology and Laboratory Medicine [G. C., D. S., A. P., L. I., P. S. M.], Human Genetics and Biostatistics [S. H.] Henry E. Singleton Brain Cancer Research Program [T. F. C., P. S. M.], and The Howard Hughes Medical Institute [C. L. S.], David Geffen School of Medicine, University of California Los Angeles, Los Angeles, California 90095; Department of Clinical Chemistry, University of Helsinki, Helsinki, Finland FIN-00014 [A. P.]; and Cell Signaling Technologies, Beverly, Massachusetts 01915 [K. C., B. S.]

Abstract

Deregulated signaling through the phosphatidylinositol 3′-kinase (PI3K) pathway is common in many types of cancer, including glioblastoma. Dissecting the molecular events associated with activation of this pathway in glioblastoma patients *in vivo* presents an important challenge that has implications for the development and clinical testing of PI3K pathway inhibitors. Using an immunohistochemical analysis applied to a tissue microarray, we performed hierarchical clustering and multidimensional scaling, as well as univariate and multivariate analyses, to dissect the PI3K pathway *in vivo*. We demonstrate that loss of the tumor suppressor protein PTEN, which antagonizes PI3K pathway activation, is highly correlated with activation of the main PI3K effector Akt *in vivo*. We also show that Akt activation is significantly correlated with phosphorylation of mammalian target of rapamycin (mTOR), the family of forkhead transcription factors (FOXO1, FOXO3a, and FOXO4), and S6, which are thought to promote its effects. Expression of the mutant epidermal growth factor receptor vIII is also tightly correlated with phosphorylation of these effectors, demonstrating an additional route to PI3K pathway activation in glioblastomas *in vivo*. These results provide the first dissection of the PI3K pathway in glioblastoma *in vivo* and suggest an approach to stratifying patients for targeted kinase inhibitor therapy.

Introduction

PI3K[4] is a lipid kinase that promotes diverse biological functions including cellular proliferation, survival, and motility. Considerable evidence demonstrates a role for PI3K signaling in oncogenic transformation and cancer progression (1). Deregulated PI3K signaling also provides an attractive target for therapy (2–4). The principle that kinase inhibitors can be effective treatments for some types of cancer has been demonstrated (2, 5), and PI3K pathway inhibitors are already in early clinical trials (4). Currently, our understanding of the signaling events that regulate and are regulated by PI3K signaling derives primarily from *in vitro* models (1, 6). Mouse genetic studies further demonstrate a key role for this pathway in cancer development and progression (1). Dissecting the molecular events associated with PI3K deregulation in cancer patients *in vivo* represents a critical extension of this work and has important implications for the design of "smart" clinical trials with PI3K inhibitors. Glioblastoma, the most common primary brain tumor of adults, is highly suited for this approach (7). Glioblastomas commonly contain mutations and deletions of the *PTEN* tumor suppressor gene, which negatively regulates PI3K signaling (8, 9). Up to now, assessment of multiple nodes in this pathway in routinely processed patient biopsy samples has not been possible. However, development of phosphorylation-specific antibodies that allow for detection of activated signaling molecules in paraffin-embedded biopsy tissues has enabled us to analyze the PI3K pathway in glioblastoma biopsies.

Materials and Methods

Tissue Microarray/Immunohistochemistry

We constructed a tissue array consisting of three representative 0.6-mm cores from formalin-fixed, paraffin-embedded tissue blocks from each of 45 glioblastomas. Sections were stained with monoclonal antibodies to PTEN (clone 6H2.1; Cascade Bioscience, Winchester, MA), EGFR (clone 31G7; Zymed, San Francisco, CA), and EGFRvIII (clone L8A4; a generous gift from Dr. Darrell Bigner) and phosphorylation-specific antibodies p-Akt (Ser-473) and p-FKHR (Thr-24)/p-FKHRL1 (Thr-32) that recognize phosphorylated forms of the forkhead family of transcription factors FKHR (FOXO1), FKHRL1 (FOXO3a), and AFX (FOXO4), p-mTOR (Ser-2481), p-S6 ribosomal protein (Ser-235/236), and p-44/42 mitogen-activated protein kinase (p-Erk; Thr-202/Tyr-204; Cell Signaling Technology, Beverly, MA). We performed antigen retrieval with a 0.01 M citrate buffer (pH 6) for 30 min in a pressure cooker (phosphorylation-specific antibodies), 16 min in a microwave oven (PTEN), and 25 min in a vegetable steamer (EGFRvIII). For EGFR, we used Pronase [0.03 g/ml in 0.05 M Tris buffer (pH 7.4)] at 37°C for 8 min. Peroxidase activity was quenched with 3% hydrogen peroxide in water. Primary antibodies [PTEN at 1:400, EGFR at 1:150, EGFRvIII at 1:400, p-Akt at 1:50, p-mTOR at 1:50; p-FKHR/FKHRL1/AFX (FOXO1/FOXO3a/FOXO4) at 1:50, pS6 at 1:50, and p-Erk at 1:50)] were diluted in Tris-buffered saline with 0.1% Tween and applied for 16 h at 4°C, followed by biotinylated secondary antibodies (Vector) at 1:1000 dilution for 1 h and avidin-biotin complex (Elite ABC; Vector) for 1 h. Negative control slides received normal mouse serum (DAKO) as the primary antibody. Diaminobenzidine tetrahydrochloride was used as the enzyme substrate to visualize specific antibody localization for PTEN, EGFR, and EGFRvIII; Vector NovaRed (Vector) was used for phosphorylation-specific antibodies. Slides were counterstained with Harris hematoxylin.

Scoring and Interpretation of Immunohistochemistry

PTEN. PTEN staining was scored according to a previously established scale of 0–2, which has been shown to be highly consistent (10–13). Tumor
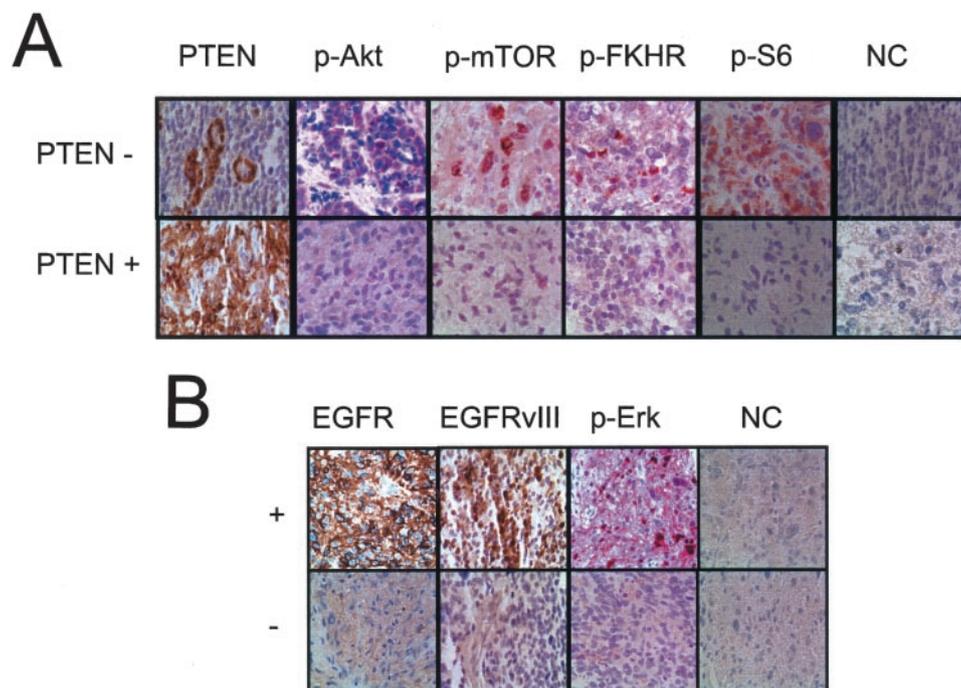
Fig. 1. Immunohistochemical analysis of the PI3K pathway. *A*, PTEN protein is lost in a subset of glioblastomas, as seen by retention of PTEN expression in the vascular endothelium with loss of PTEN in tumor cells. The PTEN-deficient tumors demonstrated phosphorylation of Akt, mTOR, FKHR, and S6. *B*, EGFR, EGFRvIII, and p-Erk were also detected by immunohistochemistry.

cells are graded as 2 if their staining intensity is equal to that of the vascular endothelium, graded as 1 if their staining intensity is diminished relative to the endothelium, and graded as 0 if staining intensity is undetectable in the tumor cells and present in the vascular endothelium (10–13). Two neuropathologists (G. C. and P. S. M.) scored the tumors independently. In addition, tumors were scored by one of the neuropathologists (P. S. M.) on two independent occasions. Both the inter-rater and the intra-rater agreement were >90%.

EGFR and EGFRvIII. Tumors demonstrating strong EGFR immunopositivity in >20% of tumor cells were considered to be positive; tumors demonstrating at least focal moderate to strong immunoreactivity for EGFRvIII were considered positive. The inter-rater and intra-rater agreements for EGFR and EGFRvIII were >90%. The anti-EGFRvIII L8A4 monoclonal antibody was generated against the fusion junction of the mutant EGFRvIII and shown to be specific for EGFRvIII, with no detectable cross-reactivity for wild-type EGFRs expressed in normal tissues or at high levels in cancer cell lines (14). However, we cannot entirely exclude the possibility that there may be some cross-reactivity with highly overexpressed wild-type EGFRs in glioblastoma tissue samples.

Phosphorylation-specific Antibodies. p-Akt, p-mTOR, p-S6, and p-FKHR were scored on a scale of 0–2 (0^+, no staining; 1^+, mild intensity cytoplasmic staining; and 2^+, strong cytoplasmic staining). For p-Akt, p-mTOR, and p-FKHR, staining of 1^+ and 2^+ was considered positive; for p-S6, staining of 2^+ was considered positive. The agreement between reviewers, as well as for the same reviewer on independent reviews, was 80% for p-Akt. It was higher for p-mTOR, p-S6, and p-FKHR, ranging from 87% for p-mTOR to 100% for p-S6. For p-Erk, tumors that focally contained greater than 5% positive nuclear staining were considered positive, as reported previously. The agreement between reviewers and for the same reviewer on independent reviews was >85%.

Statistical Analysis

We fit two multivariate logistic regression models (Table 2). First, we regressed PTEN status on p-Akt, p-mTOR, p-FKHR, p-S6, and p-Erk. In the multivariate model, only p-Akt turned out to be a significant ($P = 0.0043$) predictor of PTEN status; the odds of a case being PTEN positive when p-Akt is positive are only 0.13 (95% CI, 0.030–0.52) that of a p-Akt-negative case. Second, we regressed p-Akt status on p-FKHR family, p-S6, p-Erk, and EGFRvIII. We did not include mTOR in the model because it was highly correlated (Pearson correlation = 0.56; $P = 0.00019$) with p-FKHR and would have led to adverse multi-colinearity effects. In the multivariate model, only

p-FKHR family turned out to be a significant predictor of p-Akt status ($P = 0.015$). The odds of a case being p-Akt positive when FKHR transcription factors are phosphorylated are 3.8 times (95% CI, 1.3–11.0) that of a case with p-FKHR negative and Akt (positive *versus* negative).

The computation of the Pearson correlations and the logistic regression analysis were all carried out with the R software (15).[5] To depict the relationship between the variables, we used the R function cmdscale to arrive at a two-dimensional classical MDS plot (Fig. 2*A*). The aim of MDS is to represent dissimilarities (here, one minus the squared Pearson correlation) between points (here, variables) well. We aimed to choose a two-dimensional configuration of points that minimized a "stress" function (16). The hierarchical clustering of patients (Fig. 2*B*) was performed using publicly available Cluster and Treeview programs (publicly available from the Stanford University web site).[6] We used an uncentered correlation matrix with complete linkage to cluster the tumor samples.

Results and Discussion

We constructed a tissue microarray consisting of biopsies from 45 untreated primary glioblastoma patients. We analyzed PTEN protein expression, and we used phosphorylation-specific antibodies to assess activation of Akt, mTOR, the family of forkhead (FKHR) transcription factors (FOXO1/FOXO3a/FOXO4), and S6, which are thought to be effectors of this pathway (Fig. 1; Refs. 1, 3, 4, 8, 9, and 17). PTEN protein loss was significantly inversely correlated with Akt phosphorylation ($r = -0.58$; $P = 0.00007$), but not with Erk activation (Table 1). Akt activation was significantly correlated with p-FKHR ($r = 0.48$; $P = 0.002$) and p-mTOR ($r = 0.3$; $P = 0.067$). S6 phosphorylation was not directly associated with p-Akt but was correlated with p-mTOR and p-Erk (Table 1). Importantly, downstream of Akt, the correlation between PTEN and each successive marker diminished, suggesting a role for additional inputs into this pathway downstream of Akt.

We then fit a multivariate logistic regression model with PTEN as the outcome and p-Akt, p-FKHR, p-mTOR, p-S6, and p-Erk as the covariates (Table 2). A strong independent association between PTEN

---

[5] http://cran.r-project.org/.
[6] Stanford University website.

Table 1 *Univariate analysis*

	Pearson correlation	P
PTEN		
p-Akt	−0.58	0.00007
p-FKHR	−0.27	0.09
p-mTOR	0.003	0.98
p-S6	−0.008	0.96
p-Erk	0.07	0.66
p-Akt		
p-FKHR	0.48	0.002
p-mTOR	0.3	0.07
p-S6	0.28	0.08
p-Erk	0.13	0.43
p-S6		
p-mTOR	0.35	0.03
p-Erk	0.37	0.02
EGFR		
PTEN	−0.15	0.33
EGFRvIII	0.31	0.04
p-Erk	0.34	0.03
p-Akt	0.07	0.67
p-FKHR	0.25	0.12
p-mTOR	0.24	0.13
p-S6	0.3	0.06
EGFRvIII		
PTEN	0.13	0.41
p-Akt	−0.02	0.89
p-FKHR	0.33	0.04
p-mTOR	0.31	0.06
p-S6	0.3	0.06

and p-Akt was identified. Fitting the model for p-Akt and including p-FKHR, p-S6, and p-Erk as covariates demonstrated a significant independent association between Akt and FKHR activation. Interestingly, the association between p-Akt and p-mTOR did not quite reach significance in multivariate analysis ($P = 0.06$), despite being highly significantly correlated in univariate analysis. This potentially reflects the role for additional inputs to mTOR activation (nutrients, amino acids, cellular ATP, and phosphatidic acid), some of which may be associated with other parts of the signaling pathway.

Because our data suggested that there are additional inputs into activation of mTOR, the family of FKHR transcription factors and S6, independent of PTEN loss, we analyzed the expression of EGFR and its constitutively active mutant, EGFRvIII, which are thought to activate the PI3K pathway (18). EGFR overexpression/amplification is common in glioblastomas, and a mutant ligand independent variant (EGFRvIII) is coexpressed in approximately one-half of EGFR-amplified glioblastomas (19, 20). In our data set, EGFRvIII expression was correlated with EGFR expression ($r = 0.31$; $P = 0.04$), being seen in slightly more than one-half of the EGFR-positive tumors. EGFR expression was correlated with Erk ($r = 0.34$; $P = 0.03$) and S6 activation ($r = 0.31$; $P = 0.06$), but not with p-Akt, p-mTOR, or p-FKHR. In contrast, EGFRvIII had a strong association with phosphorylation of FKHR transcription factors, mTOR and S6. These results potentially suggest a role for EGFRvIII in activation of the PI3K pathway in the absence of PTEN protein loss and suggest an association between EGFR expression and Erk activation *in vivo*.

The results from the univariate and multivariate analyses are consistent with the presumed relationships between PTEN and other known components of the PI3K signaling pathway. Next, we asked if our data set might be used to uncover these relationships without prior knowledge of the connectivity between these proteins using MDS analysis, a form of principle component analysis. MDS is an unsupervised data analysis method that allows examination of potential relationships between variables without assuming previous knowledge of their interactions. Using this approach, the signaling molecules are plotted in two dimensions, and the distance between two molecules provides a measure of their inter-relatedness (21). PTEN protein expression and Akt activation are closely related (Fig. 2B), as

detected by the short distance between them. In contrast, p-Erk is distant from PTEN and p-Akt. Activated Akt is positioned between PTEN and p-FKHR, p-mTOR, and p-S6, suggesting that Akt is intermediate between PTEN and this pathway. Furthermore, the proximity of p-S6 to p-mTOR and p-Erk suggests potential dual activation. This unbiased approach demonstrates a pattern of inter-relationships between these signaling molecules *in vivo* that reflects our knowledge of the signaling pathway derived from *in vitro* experimental studies and raises the possibility that this form of analysis might be applied to other data sets where the connectivity between the variables is less defined (Fig. 2C).

Lastly, we asked whether these markers could provide meaningful "signatures" that can be used to stratify patients for targeted therapy. We performed hierarchical clustering of the tumors based on expression of EGFR, EGFRvIII, p-Erk, PTEN, p-AKT, p-mTOR, p-FKHR, and p-S6 to look for the emergence of molecular subsets. Two main subsets of glioblastomas were identified (main branches of the dendrogram) based on expression of PTEN protein ($P < 0.0000001$). We also identified two additional subsets of PTEN-expressing glioblastomas, based on expression of EGFR ($P = 0.00001$). One subset (branch) of the PTEN-expressing, non-EGFR-expressing tumors lacked either Erk or the PI3K pathway activation. In contrast, the EGFR-expressing subset coexpressed EGFRvIII in 14 of 16 (88%) cases, whereas, EGFRvIII was coexpressed in only 5 of 19 (26%) of the PTEN-deficient EGFR-expressing tumors ($P = 0.003$). This suggests that EGFRvIII may be selected for in the absence of PTEN loss (as a way to activate PI3K) and is line with a mouse genetic model demonstrating a key role for combined deregulation of the Ras and PI3K pathways in the development of glioblastomas (22). This approach may provide a potential design for stratifying patients for therapy with PI3K pathway inhibitors, alone or in combination with Ras/Erk and EGFR inhibitors.

In conclusion, we have demonstrated an approach to analyzing the PI3K pathway in glioblastoma patients *in vivo*. We have shown that this pathway can be assessed in routinely processed patient samples, and we have demonstrated that the signaling relationships suggested *in vitro* are reflected in glioblastoma patients *in vivo*. We have shown that loss of the tumor suppressor protein PTEN is highly correlated with activation of Akt, which is significantly correlated with phosphorylation of downstream effectors mTOR, the FKHR family of transcription factors, and S6. We have also presented data suggesting that the mutant EGFR, EGFRvIII, may also potentially activate this pathway in glioblastomas with no loss of PTEN protein. We have used MDS to analyze the relationship between signaling molecules *in vivo*, suggesting that MDS might have utility in the analysis of data sets where pathway connectivity is less defined. Finally, we have provided an approach to identify subsets of glioblastoma patients based on these "pathway signatures" that may potentially be useful for stratifying patients for targeted kinase inhibitor therapy. This approach can

Table 2 *Multivariate logistic regression analysis*

Outcome	Covariates	Odds ratio	95% CI	P
PTEN				
	p-Akt	0.13[a]	(0.03–0.52)	0.0043
	p-mTOR	0.54	(0.061–4.80)	0.58
	p-FKHR	1.10	(0.24–4.60)	0.94
	p-S6	5.00	(0.470–53.00)	0.18
	p-Erk	0.88	(0.092–8.30)	0.91
Akt				
	p-FKHR	3.80	(1.30–11.0)	0.015
	p-s6	1.70	(0.57–5.20)	0.34
	p-Erk	0.64	(0.11–3.7)	0.62
	EGFRvIII	0.33	(0.062–1.7)	0.19

[a] Odds of a tumor being PTEN deficient if it is p-Akt positive are 7.7 times (1/0.13) greater than if it is p-Akt negative.
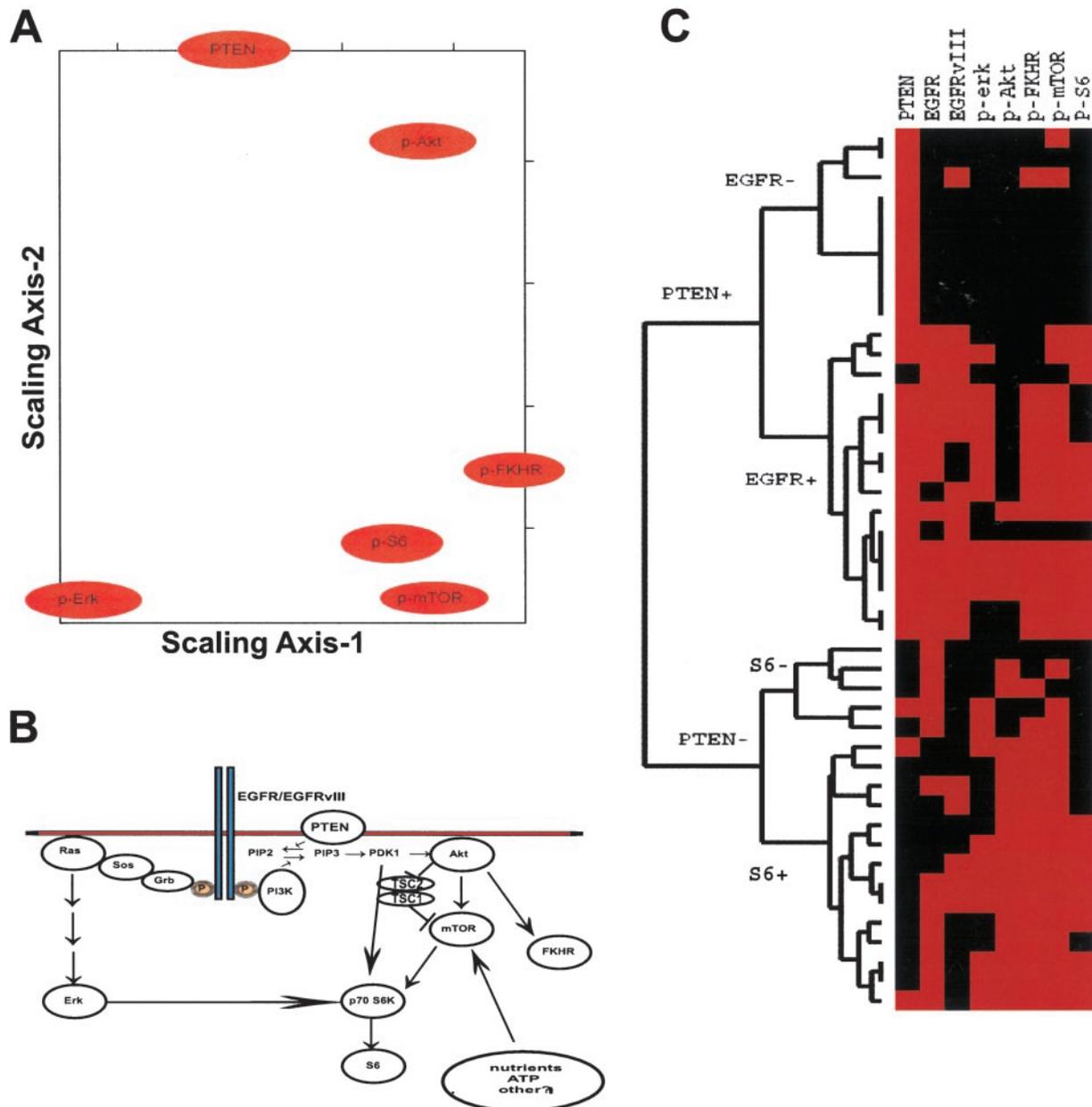
2744

Fig. 2. Demonstration of the inter-relationships between signaling molecules *in vivo*. *A,* MDS analysis shows that PTEN protein and Akt phosphorylation are tightly linked and that FKHR family transcription factors, mTOR, and S6 phosphorylation are linked to Akt and associated with each other. The location of S6 between Erk and mTOR suggests dual activation. *B,* conventional PI3K signaling pathway diagram derived from *in vitro* studies. *C,* hierarchical clustering of glioblastoma patients based on pathway signatures. Two main subsets (branches) emerge from this analysis based on PTEN expression ($P < 0.0000001$). There are also two subsets of PTEN-expressing glioblastomas; one is enriched for EGFR expression ($P = 0.00001$). The PTEN-expressing, non-EGFR-expressing tumors generally lack PI3K and Erk signaling. EGFRvIII is coexpressed with EGFR in nearly all of the PTEN-expressing tumors but in only 26% of tumors lacking PTEN ($P = 0.003$).

be applied to routinely processed patient biopsies; therefore, it may potentially have wide clinical utility. As we move from tissue arrays to patient biopsy slides, we will need to begin to assess how intratumor molecular heterogeneity impacts pathway activation, and we will need to develop controls and standards that can be applied across diagnostic laboratories. Because the key challenge for cancer therapy will be to match the right pathway inhibitor or combination of inhibitors to the right patient, this approach may have important clinical implications.

References

1. Vivanco, I., and Sawyers, C. L. The phosphatidylinositol 3-kinase AKT pathway in human cancer. Nat. Rev. Cancer, *2:* 489–501, 2002.
2. Sawyers, C. L. Rational therapeutic intervention in cancer: kinases as drug targets. Curr. Opin. Genet. Dev., *12:* 111–115, 2002.
3. Neshat, M. S., Mellinghoff, I. K., Tran, C., Stiles, B., Thomas, G., Petersen, R., Frost, P., Gibbons, J. J., Wu, H., and Sawyers, C. L. Enhanced sensitivity of PTEN-deficient tumors to inhibition of FRAP/mTOR. Proc. Natl. Acad. Sci. USA, *98:* 10314–10319, 2001.
4. Hidalgo, M., and Rowinsky, E. K. The rapamycin-sensitive signal transduction cascade as a target for cancer therapy. Oncogene, *19:* 6680–6686, 2000.
5. Druker, B. J. Perspectives on the development of a molecularly targeted agent. Cancer Cell, *1:* 31–36, 2002.
6. Blume-Jensen, P., and Hunter, T. Oncogenic kinase signaling. Nature (Lond.), *411:* 355–365, 2001.
7. Mischel, P. S., and Cloughesy, T. F. Targeted molecular therapy of glioblastoma. Brain Pathol., *13:* 52–61, 2003.
8. Ermoian, R. P., Furniss, C. S., Lamborn, K. R., Basila, D., Berger, M. S., Gottschalk, A. R., Nicholas, M. K., Stokoe, D., and Haas-Kogan, D. A. Dysregulation of PTEN and protein kinase B is associated with glioma histology and patient survival. Clin. Cancer Res., *8:* 1100–1106, 2002.
9. Davies, M. A., Lu, Y., Sano, T., Fang, X., Tang, P., LaPushin, R., Koul, D., Bookstein, R., Stokoe, D., Yung, W. K., Mills, G. B., and Steck, P. A. Adenoviral

transgene expression of MMAC/PTEN in human glioma cells inhibits Akt activation and induces anoikis. Cancer Res., *58:* 5285–5290, 1998.

10. Gimm, O., Perren, A., Weng, L. P., Marsh, D. J., Yeh, J. J., Ziebold, U., Gil, E., Hinze, R., Delbridge, L., Lees, J. A., Mutter, G. L., Robinson, B. G., Komminoth, P., Dralle, H., and Eng, C. Differential nuclear and cytoplasmic expression of PTEN in normal thyroid tissue, and benign and malignant epithelial thyroid tumors. Am. J. Pathol., *156:* 1693–1700, 2000.

11. Perren, A., Komminoth, P., Saremaslani, P., Matter, C., Feurer, S., Lees, J. A., Heitz, P. U., and Eng, C. Mutation and expression analyses reveal differential subcellular compartmentalization of PTEN in endocrine pancreatic tumors compared to normal islet cells. Am. J. Pathol., *157:* 1097–1103, 2000.

12. Perren, A., Weng, L. P., Boag, A. H., Ziebold, U., Thakore, K., Dahia, P. L., Komminoth, P., Lees, J. A., Mulligan, L. M., Mutter, G. L., and Eng, C. Immuno-histochemical evidence of loss of PTEN expression in primary ductal adenocarcinomas of the breast. Am. J. Pathol., *155:* 1253–1260, 1999.

13. Zhou, X. P., Gimm, O., Hampel, H., Niemann, T., Walker, M. J., and Eng, C. Epigenetic PTEN silencing in malignant melanomas without PTEN mutation. Am. J. Pathol., *157:* 1123–1128, 2000.

14. Wikstrand, C. J., Hale, L. P., Batra, S. K., Hill, M. L., Humphrey, P. A., Kurpad, S. N., McLendon, R. E., Moscatello, D., Pegram, C. N., Reist, C. J., *et al.* Monoclonal antibodies against EGFRvIII are tumor specific and react with breast and lung carcinomas and malignant gliomas. Cancer Res., *55:* 3140–3148, 1995.

15. Ihaka, R., and Gentleman, R. R: a language for data analysis and graphics. J. Comput. Graphical Statistics, *5:* 299–314, 1996.

16. Cox, T. F., and Cox, M. A. A. Multidimensional Scaling. United Kingdom: CRC Press, 2001.

17. Burgering, B. M., and Kops, G. J. Cell cycle and death control: long live Forkheads. Trends Biochem. Sci., *27:* 352–360, 2002.

18. Nagane, M., Lin, H., Cavenee, W. K., and Huang, H. J. Aberrant receptor signaling in human malignant gliomas: mechanisms and therapeutic implications. Cancer Lett., *162* (Suppl.)*:* S17–S21, 2001.

19. Ekstrand, A. J., Sugawa, N., James, C. D., and Collins, V. P. Amplified and rearranged epidermal growth factor receptor genes in human glioblastomas reveal deletions of sequences encoding portions of the N- and/or C-terminal tails. Proc. Natl. Acad. Sci. USA, *89:* 4309–4313, 1992.

20. Liu, W., James, C. D., Frederick, L., Alderete, B. E., and Jenkins, R. B. PTEN/MMAC1 mutations and EGFR amplification in glioblastomas. Cancer Res., *57:* 5254–5257, 1997.

21. Venables, W. N., and Ripley, B. D. Modern Applied Statistic with S-Plus. New York: Springer, 1999.

22. Holland, E. C., Celestino, J., Dai, C., Schaefer, L., Sawaya, R. E., and Fuller, G. N. Combined activation of Ras and Akt in neural progenitors induces glioblastoma formation in mice. Nat. Genet., *25:* 55–57, 2000.

Analysis of the Phosphatidylinositol 3′-Kinase Signaling Pathway in Glioblastoma Patients *in Vivo*

Gheeyoung Choe, Steve Horvath, Timothy F. Cloughesy, et al.

Updated version	Access the most recent version of this article at: http://cancerres.aacrjournals.org/content/63/11/2742

Cited articles	This article cites 19 articles, 6 of which you can access for free at: http://cancerres.aacrjournals.org/content/63/11/2742.full#ref-list-1
Citing articles	This article has been cited by 78 HighWire-hosted articles. Access the articles at: http://cancerres.aacrjournals.org/content/63/11/2742.full#related-urls

E-mail alerts	Sign up to receive free email-alerts related to this article or journal.
Reprints and Subscriptions	To order reprints of this article or to subscribe to the journal, contact the AACR Publications Department at pubs@aacr.org.
Permissions	To request permission to re-use all or part of this article, use this link http://cancerres.aacrjournals.org/content/63/11/2742. Click on "Request Permissions" which will take you to the Copyright Clearance Center's (CCC) Rightslink site.